

SURVEY

2TSS: Two-Tier Semantic Segmentation Framework With Enhancement for Hotspot Detection of Solar Photovoltaic Thermal Images

NURUL HUDA ISHAK¹, IZA SAZANITA ISA¹, (Member, IEEE),
MUHAMMAD KHUSAIRI OSMAN¹, MOHD SHAWAL JADIN²,
KAMARULAZHAR DAUD¹, AND MOHD ZULHAMDY AB HAMID¹

¹Electrical Engineering Studies, Universiti Teknologi MARA, Permatang Pauh Campus, Penang 13500, Malaysia

²Faculty of Electrical and Electronics Engineering Technology, Universiti Malaysia Pahang Al-Sultan Abdullah, Pekan, Pahang 26600, Malaysia

Corresponding author: Iza Sazanita Isa (izasazanita@uitm.edu.my)

This work was supported by the Ministry of Higher Education through Fundamental Research Grant Scheme (FRGS) under Grant FRGS/1/2023/ICT02/UITM/02/12.

ABSTRACT Recently, intelligence-based hotspot detection has been widely used in solar photovoltaic (PV) image applications. However, the semantic segmentation approach has limitations in terms of accuracy, particularly for hotspot thermal images. This study introduces a novel method based on Two-tier Semantic Segmentation (2TSS) framework explicitly aimed at enhancing hotspot detection in thermal images of PV modules. The proposed method is designed with two subsequent stages of segmentation models, including image pre-processing at the initial of the framework. The first tier of segmentation distinguishes between solar PV modules and the background, whilst the second tier enhances the hotspot localization region. This research enhances comprehension of multi-tier segmentation architectures in deep learning, focusing on optimizing performance for solar energy systems through comparative analysis of semantic models. Three different segmentation models, namely U-Net, ResNet 18 and ResNet 50 were tested. The ResNet 50 model demonstrated superior segmentation performance across both tiers with 98% and 85% accuracy respectively. In summary, the proposed method demonstrates that applying a combined enhancement algorithm prior to training for hotspot segmentation promotes superior performance with an accuracy improvement of 2.26% over the non-enhancement approach.

INDEX TERMS Two-tier, semantic segmentation, solar PV, hotspot, detection.

I. INTRODUCTION

The rising global need for renewable energy has placed solar PV systems at the front of sustainable energy generation [1]. Solar PV technology is pivotal in reducing dependence on fossil fuels and mitigating environmental impacts. Even with this, the efficacy and durability of solar systems can be markedly undermined by numerous faults. Hotspot is the region that has the highest thermal accumulation within PV modules [2]. Immediate and precise identification of these hotspots is crucial for maximizing system efficiency, minimizing energy loss, and improving the operational lifespan

The associate editor coordinating the review of this manuscript and approving it for publication was Furkan Ahmad¹.

of solar PV installations. Figure 1 shows an example of the hotspots on the solar PV panel.

Therefore, developing effective methods for hotspot detection has become a critical focus in solar energy research, with the potential to significantly reduce environmental footprint [3]. Additionally, deep-learning approaches encounter challenges such as low accuracy, high false-positive rates, and inefficiencies in large-scale PV deployments due to variations in image quality and environmental conditions.

This research addresses two key challenges in hotspot segmentation for solar PV systems: low detection accuracy and poor performance under complex shading conditions [4]. Traditional semantic segmentation techniques must be better suited to handle the complex and noisy thermal images

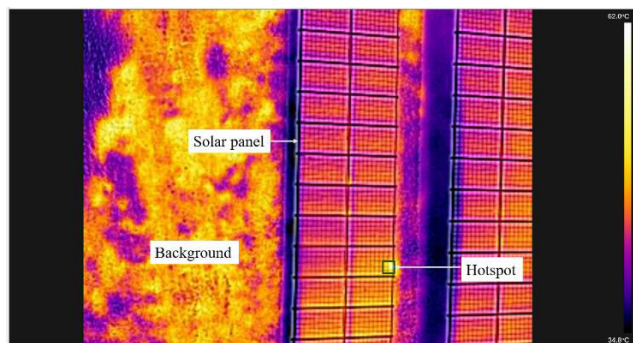


FIGURE 1. An example of the existence of hotspots on solar panels captured using thermal camera.

produced in real-world PV environments [5]. The imprecision in identifying specific hotspot areas frequently results in misdiagnosis. This can lead to inappropriate maintenance or, more critically, the oversight of severe issues. This study proposes a novel Two-tier Semantic Segmentation (2TSS) model to overcome these limitations. The first tier conducts coarse segmentation to identify solar PV panels, while the second tier refines these regions for precise hotspot detection. This innovative approach enhances detection accuracy, reduces false positives, and improves computational efficiency, enabling scalable and real-time implementations for large-scale PV systems.

II. HOTSPOT DETECTION AND CHALLENGES

The complexity of thermal image processing and the variations in operational and environmental factors make identifying hotspots in solar PV systems extremely challenging [2]. The accuracy and effectiveness required for real-time hotspot detection are sometimes lacking in conventional methods, such as human inspections and basic image processing algorithms. These systems also have problems with false positives, scalability for large PV farms, and the inability to adapt to fault patterns that change over time [6].

Advanced methods that use image processing, machine learning, and semantic segmentation have emerged to overcome these limitations. These technologies provide improved detection capabilities that minimize processing errors and time [7], [8]. Developing an efficient two-tier semantic segmentation framework aims to address these issues by combining hierarchical processing with cutting-edge deep learning techniques. Subsequently, it offers improved hotspot detection and mitigation solutions in solar PV systems. These technologies enhance detection capabilities, reducing processing errors and time while facilitating accurate classification and identification of hotspots. Although these sophisticated frameworks offer significant potential, they are often accompanied by challenges related to integration, high processing power demands, and the need for large annotated datasets.

A. HOTSPOT PHENOMENA IN SOLAR PHOTOVOLTAIC SYSTEMS

Hotspot formation in solar PV systems significantly impacts energy conversion efficiency, which also poses significant risks to the safety and longevity of PV modules [9]. Hotspots are areas within a PV module that experience elevated temperatures due to localized electrical mismatches resulting from partial shading, intrinsic module defects or other operational inconsistencies. These hotspots could cause thermal stress and worsen the degradation of solar PV cells if they are not identified [2]. If these hotspots are not detected, this may result in thermal stress and further deterioration of the solar PV cells. In the extreme, it can result in irreversible damage or even fires. Hence, timely detection of hotspots is crucial for the proper operation of solar PV systems. Moreover, reducing the burden of maintenance would ensure safe operation.

Recent research concentrates on creating effective detection methods to quickly and accurately identify real-time hotspots to tackle issues of energy loss and operational inefficiencies [10], [11], [12]. Diverse methodologies have been developed to identify hotspots in solar panels. This encompasses image processing techniques that utilize thermal imaging to identify abnormal temperature patterns. Machine learning techniques use data patterns to classify hotspot zones [13]. Artificial intelligence (AI) algorithms also make automatic and predictive monitoring easier. These sophisticated detection techniques reduce the effect of hotspots on system performance by enabling early diagnosis and intervention. This research investigates recent advancements in hotspot detection technologies by analysing the strengths and weaknesses of various methodologies. In addition, it emphasizes the promise of integrated solutions that merge image processing, machine learning, and artificial intelligence to develop precise and efficient hotspot detection systems for solar PV installations.

Despite the availability of various techniques for detecting hotspots in PV modules, significant challenges still need to be resolved. Conventional image processing techniques like thresholding and edge detection frequently struggle to effectively segment intricate thermal images because of noise, shading effects, and environmental factors [14]. These methods require enhanced precision, particularly in large-scale PV installations where variability in image quality can lead to high false-positive rates. More advanced approaches based on deep learning and convolutional neural networks (CNNs) have been introduced, showing improvements in detection accuracy. However, these models often face limitations in practical applications as they are computationally intensive [15], require large datasets for training [16], and may need to generalize better across different PV installations or environmental conditions [17]. As a result, existing models face challenges in delivering real-time, accurate, and reliable hotspot detection, which is critical for the efficient operation of large PV systems.

In conclusion, recent machine learning and image processing progress has improved hotspot detection in solar PV systems. However, practical application remains constrained in various real-world settings due to accuracy, data requirements, and model adaptability issues. Further development is required to develop lightweight and adaptive models to effectively control large-scale solar PV systems. These models should maintain high detection accuracy under varying environmental conditions, minimize false positives, and operate efficiently in real-time. Solving these issues is essential to developing scalable, dependable hotspot detection systems that complement the world's increasing reliance on solar energy.

B. HOTSPOT DETECTION USING MACHINE LEARNING AND IMAGE PROCESSING

Identifying hotspots in solar PV systems has been substantially improved through developments in image processing, machine learning, infrared thermography, and AI. Infrared thermography (IRT), a non-invasive monitoring technique, has become a cornerstone in identifying thermal anomalies across PV modules [18]. Significant analysis and machine learning approaches are combined in IRT-based systems to effectively identify hotspots while reducing the need for large, labelled datasets. Furthermore, CNNs have demonstrated improved hotspot identification performance because they extract complex information from thermal images, enabling precise fault segmentation and localization. Automated fault identification and preventive maintenance are made possible by the designs' convolutional, pooling, and fully connected layers, which transform raw input data into valuable information [12].

Despite recent advancements, current systems still encounter substantial computational demands, large data sets, and restricted adaptability to varying environmental conditions and solar installations. Researchers have examined lightweight models and optimization strategies such as knowledge distillation and feature compression to overcome these limitations and improve computational efficiency [19], [20], [21]. Additionally, real-time hotspot detection systems that employ I-V characteristics and current fluctuations have facilitated the early diagnosis of defects and easy integration with existing PV arrangements [22]. Together, these innovations improve the reliability and scalability of PV system diagnostics, paving the way for more efficient and cost-effective maintenance strategies in large-scale installations.

C. IMAGE ENHANCEMENT FOR HOTSPOT DETECTION

Image enhancement is essential for improving the quality of thermal images, especially in PV inspection systems where resolution is frequently low, and noise levels are high. Thermal images are often low contrast and noisy, making it challenging for automated algorithms and human interpretation to detect faults like hotspots accurately. As a

result, enhancement techniques are frequently applied as a pre-processing step to improve the visual quality and facilitate better segmentation or classification performance.

To increase contrast, traditional techniques such as Histogram Equalization (HE) and Adaptive Histogram Equalization (AHE) may produce noise or over-enhancement in uniform areas. Advanced techniques include multi-scale fusion methods, wavelet-based enhancement, Retinex models, and guided filtering. A study in [23] employed multi-scale directed filtering with CLAHE to enhance thermal infrared images, improving contrast and image information retention. Similarly, the method proposed in [24] applied CLAHE enhancement across multiple color spaces, including LAB and HSV, followed by adaptive fusion. This two-stage process significantly enhances the contrast and detail visibility of thermal infrared images under low-illumination conditions.

The combination of CLAHE and non-local means (NLM) denoising has shown positive results because it successfully strikes a compromise between noise reduction and contrast enhancement. CLAHE enhances local contrast in non-uniformly illuminated thermal images, making subtle structural differences more visible while preventing excessive brightness distortion [25]. NLM filtering simultaneously eliminates noise while maintaining critical edges and textures by utilizing the self-similarity of image patches, exhibiting robust performance across diverse noise levels [26]. A recent study in [27] introduced a hybrid enhancement method combining CLAHE, Wavelet Transform, and NLM denoising, significantly improving image clarity and structural detail in medical datasets such as FracAtlas and MURA. Even though this study concentrated on medical imaging, the technique is applicable to thermal PV applications due to its capacity to improve noisy and low-contrast data. The complementary strengths of CLAHE and NLM continue to support their integration in hybrid pipelines for enhanced image clarity and segmentation readiness.

The literature supports the CLAHE-NLM hybrid as a practical and pragmatic enhancement method that reconciles contrast enhancement with noise reduction. Its capacity to amplify complex elements while maintaining essential image structures made it especially appropriate for thermal PV applications, where segmentation precision is significantly reliant on the quality of the input image. Applying this dual-stage enhancement prior to a two-tier semantic segmentation process can significantly improve the accuracy and reliability of hotspot detection.

D. SEMANTIC SEGMENTATION METHOD

In computer vision, semantic segmentation refers to partitioning an image into different regions where each pixel is classified to represent a specific class or object [28]. Semantic segmentation differs from image classification, wherein there is only one label for the whole image, and from object detection, which identifies multiple objects along with their locations. Semantic segmentation provides a pixel-level

understanding of the scene. It is beneficial in applications with critical detailed image analysis, such as medical imaging, satellite remote sensing, and autonomous driving, where identifying regions is imperative. Figure 2 illustrates semantic segmentation scenes of solar PV modules.

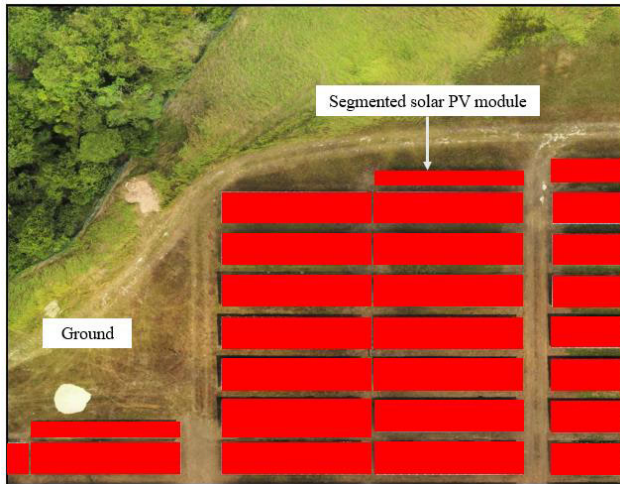


FIGURE 2. Semantic images for solar PV panels.

Deep learning methods have revolutionized semantic segmentation by developing robust approaches for extracting detailed information from images. Naturally, CNNs lie at the heart of these methods, as they can learn high-level and fine-grained features within an image in a very automatic manner. Advanced networks such as FCN and other encoder-decoder architectures enable the handling of spatial information in a highly effective manner that is quite suitable for pixel-wise tasks. These models are designed to capture complex visual patterns and textures that will be very helpful and crucial in segmenting diverse regions of an image into true and accurate pieces. This work involved training and testing two types of CNN models, U-Net and ResNet to evaluate their performance. Figure 3 illustrates the basic structure of CNN-based classification, constructed to precisely and efficiently detect solar PV panels and hotspots in thermal imagery.

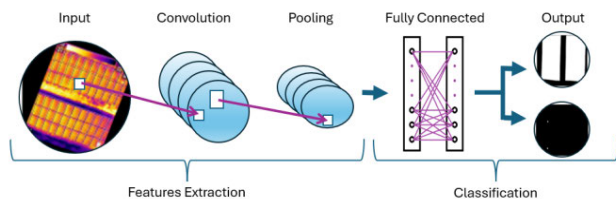


FIGURE 3. Deep learning architecture.

Semantic segmentation in an industrial application for PV plant monitoring has grown since these methods can detect hotspots or any other anomaly quite accurately down to the pixel level. The two-tier segmentation approach which integrates coarse and fine segmentation in PV systems, may

enhance the efficiency and accuracy of hotspot detection. The first tier, a coarse segmentation tier, provides regions of interest with a reduced computational load due to filtering out areas irrelevant for monitoring. Subsequently, the fine segmentation tier will deliver accurate delineation of each hotspot. This will keep PV monitoring at a hierarchical real-time speed and accuracy.

1) U-NET

U-Net is a popular encoder-decoder model specifically developed for semantic segmentation, designed to capture both the spatial and contextual details within an image [29], [30]. It is structured as a “U” shape, where the contracting path (encoder) gradually reduces the spatial dimensions while extracting high-level features, and the expanding path (decoder) progressively restores the spatial dimensions to the original resolution. The defining characteristic of U-Net is its use of skip connections between corresponding encoder and decoder layers, which help preserve fine spatial details by combining low-level and high-level features. This makes U-Net particularly effective in tasks that require precise boundary delineation, such as segmenting medical or thermal images in PV applications [31], [32].

2) RESNET

ResNet, or Residual Network, is a deep CNN that addresses the problem of vanishing gradients in very deep networks, allowing for the construction of extremely deep architectures without degradation in performance [29], [33]. ResNet introduces residual blocks, where each block has skip connections that add the input directly to the output of a few convolutional layers. This enables the network to identity mappings and focus on refining features, leading to efficient feature extraction across layers [34]. Due to its deep structure and ability to handle complex data representations, ResNet is often used as a backbone in semantic segmentation tasks.

E. SEMANTIC SEGMENTATION USING DEEP LEARNING FOR HOTSPOT DETECTION

Recent advancements in deep learning architectures, particularly CNNs, have markedly improved the accuracy and efficiency of semantic segmentation [35]. Consequently, it has become an essential instrument in multiple fields, particularly solar PV hotspot detection [36], [37], [38]. Semantic segmentation is essential for detecting defects in solar PV systems, including hotspots, cracks, and dirt accumulation. Accurate detection of anomalies is crucial for optimizing the performance and longevity of solar PV modules. Thermal imaging, commonly employed for examining solar PV systems, presents distinct issues caused by temperature gradients, low resolution, and fluctuations in noise [7]. Semantic segmentation algorithms tackle these difficulties by accurately identifying hotspots and assessing their severity, thus enabling prompt maintenance and minimizing energy losses. Recent research has shown that deep learning-based

segmentation models effectively automate the analysis of PV thermal images, surpassing previous methods in accuracy and reliability [39].

Semantic segmentation has performed better in challenging image processing settings when combined with cutting-edge methods, including transfer learning, attention mechanisms, and multi-scale feature extraction [40]. Transfer learning allows pre-trained models to be fine-tuned for specific applications, reducing computational costs and the need for extensive labelled datasets. However, attention mechanisms help the model to focus on relevant regions, boosting segmentation accuracy in cluttered or ambiguous environments. These advances in PV systems can recognize several problems concurrently, offering a complete module health image.

Despite its impressive development, semantic segmentation must improve with computing needs, extensive labelled datasets, and generalization across varied settings [41]. Emerging trends, such as synthetic data generation, weakly supervised, and federated learning address these limitations. In solar PV applications, integrating semantic segmentation with domain-specific knowledge, including thermography and material science, can significantly improve the robustness and applicability of these models. With the increasing demand for efficient and sustainable energy solutions, semantic segmentation will remain fundamental for strengthening solar PV system diagnostics and monitoring.

Semantic segmentation has been increasingly utilized in solar PV systems to detect hotspots by leveraging thermal or infrared imaging, which identifies localized regions of elevated temperature indicative of potential faults. Early methods used traditional image processing techniques, such as thresholding and morphological operations to segment defective areas [42]. However, these methods often require help with noise and variable lighting conditions. They also faced challenges with complex backgrounds in large PV arrays, resulting in inaccurate results. More recently, deep learning-based approaches have gained traction with models such as U-Net, SegNet, and Mask R-CNN employed for hotspot detection.

Recent advancements in hotspot detection for solar PV systems highlight a significant emphasis on improving accuracy, efficiency, and scalability. Methods like lightweight deep learning models namely YOLO [43], [44], [45], [46], [47] UAV-based imaging [48], [49], and hybrid approaches [4], [50] combine segmentation, detection, and performance analysis to enhance reliability. These approaches tackle issues such as extensive solar PV arrays and the optimization of operational efficiency. The incorporation of advanced technologies guarantees accurate detection, lowers maintenance expenses, and facilitates scalable solutions for extensive PV installations, indirectly driving improvement in sustainable and efficient solar energy systems.

The current trend in detecting and segmenting hotspot is shown in Table 1. This table summarizes recent methodologies and findings in detecting hotspots and faults in solar PV

systems. It highlights diverse approaches, such as a novel data-driven technique using manifold learning (NSE). This technique and the Otsu thresholding method improve sensitivity and real-time detection efficiency. A deep learning framework based on YOLO demonstrates the importance of automated segmentation for PV panel inspection. Additionally, fault detection combining neural networks (FBPNN) and SVM exhibits high accuracy, surpassing other methods. Finally, the Deep Solar PV Refiner utilizes advanced deep learning techniques, improving solar PV segmentation in satellite data and outperforming existing standards. These methods collectively advance automated PV fault detection and monitoring capabilities.

F. MOTIVATION FOR A TWO-TIER APPROACH

The limitations of current hotspot segmentation methods highlight the need for a more robust and efficient solution. A 2TSS approach presents a promising alternative by leveraging the strengths of both coarse and fine-grained segmentation techniques. The first tier of the 2TSS framework performs coarse segmentation to rapidly identify potential regions of interest, filtering out irrelevant background information. The second tier then refines these regions, focusing on accurately detecting and localizing hotspots with higher precision. This hierarchical approach not only improves detection accuracy but also reduces computational load by minimizing the need for complex calculations on the entire image. Additionally, the two-tier structure allows for better generalization across varying environmental conditions, making it more suitable for real-world applications in large-scale PV installations.

This study aims to develop and validate the 2TSS model as a novel solution for improving hotspot detection in solar PV systems. The primary objective is to enhance detection accuracy while maintaining computational efficiency, thereby addressing the limitations of current methods. The specific contributions of this research include:

- i. The introduction of a two-tier semantic segmentation framework tailored for the detection of hotspots in solar PV systems.
- ii. A thorough evaluation of the 2TSS model's performance compared to existing segmentation techniques, demonstrating its superiority in terms of both accuracy and processing speed.
- iii. The development of a computationally efficient method that enables real-time monitoring and detection, making it practical for large-scale PV plants.

III. PROPOSED METHOD

In this study, the proposed 2TSS framework for hotspot detection in solar PV thermal images was developed and evaluated using MATLAB. The experiments were conducted on a high-performance personal computer (PC) running the Windows 11 Operating System (OS) with the following hardware specifications: an Intel i5-12400 @ 2.50 GHz processor, 16 GB of RAM, and a GEFORCE RTX 3060 GPU with 8 GB

TABLE 1. The current trend in hotspot detection and segmentation.

| Study | Methodology | Main Finding | Limitations |
|--|--|---|--|
| Tendency-Aided Data-Driven Method for Hot Spot Detection in Solar PV Systems. [52] | <ul style="list-style-type: none"> Developed a new data-driven method called neighbourhood slowest embedding (NSE) based on manifold learning. The NSE-based method has the advantages of increased sensitivity, high computational efficiency for real-time detection, and the ability to be applied without mathematical models or expert knowledge. | <ul style="list-style-type: none"> The method for detecting hot spots based on the NSE has demonstrated improved sensitivity in solar PV systems. The NSE method demonstrates high computational efficiency, facilitating real-time detection of hot spots. | <ul style="list-style-type: none"> Reliance on the NSE method may require a significant amount of data to train effectively, which can be challenging in environments with limited labelled datasets. The method's performance may degrade in highly dynamic or noisy operational conditions, reducing its robustness. |
| Hotspot Detection in Solar PV Module using Otsu Thresholding Method. [53] | <ul style="list-style-type: none"> The images were segmented using the Otsu thresholding method to identify hotspots in the solar PV modules. | <ul style="list-style-type: none"> Achieved an average accuracy of 92.16% in detecting hotspots at solar PV modules. | <ul style="list-style-type: none"> Thresholding techniques are sensitive to noise and variations in lighting conditions, which can lead to inaccurate segmentation in real-world thermal images. |
| A deep learning-based approach for detecting panels in solar PV plants. [54] | <ul style="list-style-type: none"> A convolutional neural network (CNN) framework called YOLO detected and segmented PV panels from images. The YOLO-based PV panel detection method was evaluated quantitatively on a benchmark dataset and compared to existing approaches. | <ul style="list-style-type: none"> Segmenting the PV panels is crucial for automatically detecting hot spots and faults in PV plants using aerial thermal imaging. | <ul style="list-style-type: none"> Deep learning models like YOLO are computationally intensive, making real-time deployment on resource-constrained devices challenging. It requires extensive labelled datasets to be generalized effectively across different PV installations and environmental conditions. |
| Solar PV's Micro Crack and Hotspots Detection Technique Using NN and SVM. [55] | <ul style="list-style-type: none"> For fault classification, Feed-Forward-Back Propagation Neural Network (FBBPNN) and Support Vector Machine (SVM) techniques were used. | <ul style="list-style-type: none"> The SVM technique exhibited a promising result with an average accuracy of 99%, outperforming the feed-forward back propagation neural network technique which had an average accuracy of 87%. | <ul style="list-style-type: none"> The method's accuracy may decline when handling complex and highly variable defect patterns. |
| Deep solar PV refiner: A detail-oriented deep learning network for refined segmentation of solar PV areas from satellite imagery. [56] | <ul style="list-style-type: none"> A new deep learning network, "Deep Solar PV Refiner," has been developed to enhance PV segmentation from satellite imagery. The network is optimized using transfer learning, synthetic data strategy, hybrid loss functions, and ablation experiments. | <ul style="list-style-type: none"> The optimized network outperforms benchmark models, demonstrating improved performance in segmenting PV areas using satellite imagery. | <ul style="list-style-type: none"> Dependency on high-quality satellite imagery and transfer learning strategies may limit its applicability in regions with low-resolution imaging data. |

memory. The 2TSS framework integrates hierarchical segmentation, where the first tier performs coarse segmentation to identify potential hotspot regions, and the second tier refines these detections with precise pixel-level localization. Deep learning toolkits and MATLAB image processing components implement unique designs like U-Net and ResNet, guaranteeing efficient computation and enhanced segmentation accuracy. The overall cost associated with this project's development amounts to approximately 10,000 USD, which is fully funded through a research grant. This cost includes the acquisition of software and hardware, data collection, expert consultation, and model validation.

Figure 4 illustrates the overall workflow of this study. The overall workflow outlines a multi-stage process for detecting hotspots in solar PV thermal images, beginning with image acquisition that includes labelled ground truth data. In pre-

processing, images are labelled and resized. The workflow then applies a two-tiered segmentation approach: the first tier distinguishes PV panels from the background, while the second tier identifies hotspots within the PV area. Finally, system performance is evaluated using metrics to assess the accuracy and effectiveness of hotspot detection in the segmented PV regions.

A. IMAGE ACQUISITION

The dataset used for this study consists of thermal images collected from a solar farm in Kelantan, Malaysia. The type of image used in this research is depicted in Figure 5. This study's image acquisition process involves capturing or procuring images of solar PV panels or farms using aerial imaging. Aerial imagery by drones or satellites shows solar PV installations from a bird's view. Images are captured at

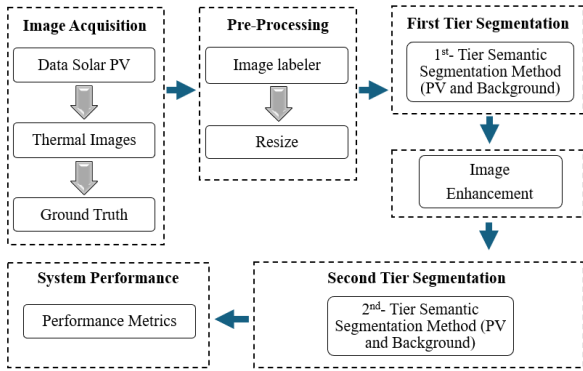


FIGURE 4. The overall workflow of proposed 2TSS segmentation framework.

low-altitude overviews using digital or specialized infrared cameras. This ensures that every single PV panel is inspected and thoroughly examined. The dataset was collected at the solar farm, Kelantan, Malaysia at an altitude of 15 meter. Figure 6 presents the height for the image capture procedure. This height is significant because it makes a complete solar PV array visible, thus ensuring comprehensive data collection.

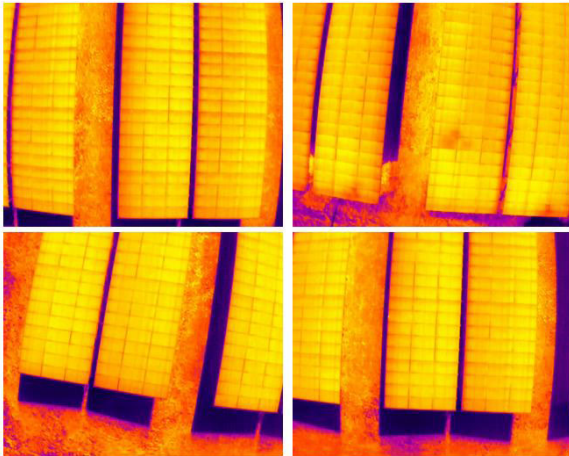


FIGURE 5. Example of solar PV thermal images (in sRGB format) captured by drone.

A Parrot ANAFI thermal camera, shown in Figure 7, was used to capture the image. The camera recorded images at a resolution of 72 dpi. The images were captured between 1st February 2020 and 31st January 2021 on clear sunny days (11 a.m. to 1 p.m.). According to the GPS data embedded in the EXIF metadata, the images were captured starting at approximately 5.9924° N, 102.1099° E and ending at approximately 5.9916° N, 102.1098° E. All images in the dataset were stored in the sRGB (Standard Red, Green, Blue) colour space, which is widely used for digital imaging applications. The thermal data from these dataset images indicate an average temperature of roughly 307.58 Kelvin (around 34.43°). At the same time, an average irradiance ranges from



FIGURE 6. Acquisition of height for the image capture procedure.

TABLE 2. Parrot anafi thermal camera specification.

| Test detector type | FLIR Lepton 3.5 microbolometer (radiometric) |
|-------------------------------|--|
| Detector resolution | 160 x 120 |
| Photo resolution | 3264 x 2448 |
| Thermal sensitivity | Less than 0.1 °C at 30°C |
| Temperature measurement range | -20 °C to +350 °C |
| Field of view | 23° x 17° |
| Infrared spectral band | 8 μm to 14 μm |

624.72 to 805.70 W/m². Table 2 summarizes the important specifications of the camera. The thermal cameras capture infrared images that display temperature variations across the panels. This differentiates between hotspots and highly heated regions, which may indicate potential issues or faults.



FIGURE 7. Parrot Anafi thermal camera.

This dataset, containing 670 thermographic aerial images, was acquired by the Anafi Thermal camera (long wavelength) from a Parrot drone (quadcopter). Ground truth annotations were manually labelled by domain experts, marking the exact location of hotspots as regions of interest. Table 3 presents the distribution of thermal images used for model execution across two tiers of the proposed segmentation framework. In the first tier, a total of 670 images are divided into training (536), testing (67), and validation (67) sets to

TABLE 3. Dataset distribution of thermal images for model execution at both tier.

| Dataset | First tier | Second tier | |
|--------------|------------|-------------|-------------|
| | | Hotspot | Non-hotspot |
| Training | 536 | 492 | 44 |
| Testing | 67 | 61 | 6 |
| Validation | 67 | 61 | 6 |
| Total | | 670 | |

distinguish solar PV modules from the background. In the second tier, the same number of images (670) is further categorized into hotspot and non-hotspot classes, where most images represent hotspot regions. Specifically, the second tier includes 492 hotspot and 44 non-hotspot images for training, 61 hotspot and 6 non-hotspot images for testing, and 61 hotspot and 6 non-hotspot images for validation. This structured distribution ensures a consistent and focused classification process, emphasizing hotspot localization in the second tier.

B. IMAGE PRE-PROCESSING TECHNIQUES

The three primary stages of the automated technique for detecting hotspot regions in thermal images are pre-processing, segmentation, and post-processing. The pre-processing stage is essential, as it includes tasks such as image annotation and resizing as depicted in Figure 8. Labelling is identifying and designating hotspot areas for solar PV hotspots to generate dependable datasets for machine learning models. Enhancement techniques that reduce noise and improve contrast significantly increase the visibility of hotspots. These pre-processing efforts ensure precise and reliable segmentation results, laying the foundation for accurate hotspot detection and analysis.

1) IMAGE ANNOTATION

The MATLAB Image Labeler app tool is applied for image labelling and segmentation. It enables the systematic identification and labelling of specific areas within images, which is valuable for generating ground truth data for machine learning tasks. The segmentation of solar PV panels and hotspot regions begins by loading the relevant images into the Image Labeler application. Specific labels, such as “solar PV” and “hotspot,” are created within the app. Regions of interest are then manually annotated by drawing rectangles or polygons around the target areas. This manual annotation process effectively generates labeled data for subsequent analysis. Once the labelling is complete, the annotated data is exported, providing a dataset that includes both the images and their corresponding labels and coordinates (as illustrated in red box) in new images.

2) IMAGE RESIZE

Thermal images were subjected to image resizing after the labelling procedure. The purpose of resizing is to reduce the

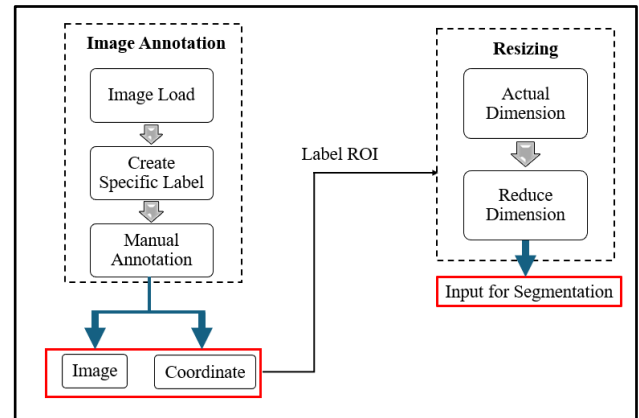
**FIGURE 8. Image pre-processing techniques involve image labelers and image resizing to generate ground truth datasets with hotspots and coordinates as ROI for segmentation phases.**

image dimension, which would be advantageous in reducing the computation cost and memory usage during the training process to guarantee a suitable patch division for the CNN. The resolution of all 670 thermal images was reduced to 224×224 from 3264×2448 to enable image segmentation. The choice of resolution size was deemed sufficient for this investigation because the image was visible without any noticeable distortion. All resized images were subsequently transmitted to the second processing stage which is image segmentation.

C. DESIGN OF TWO-TIER SEMANTIC SEGMENTATION (2TSS)

As depicted in Figure 4, the proposed 2TSS framework introduces a new segmentation approach related to solar PV systems in hotspot detection. The 2TSS framework functions in two subsequent stages to address issues related to accuracy and computational efficiency in real-time hotspot detection.

First, solar PV modules are detected. The second tier refines the initial detections to accurately locate the hotspots within the identified regions. This two-stage process leverages the strengths of both coarse and fine segmentation techniques, ensuring that the framework can balance rapid initial detection with the detailed precision necessary for accurate hotspot identification. The 2TSS architecture utilizes a hierarchical approach to improve performance relative to traditional single-tier segmentation methods. This design offers significant benefits in large-scale solar PV installations, where efficiency and precision are essential.

1) FIRST-TIER COARSE SEGMENTATION

The first tier of the 2TSS structure includes an initial segmentation phase aimed at effectively identifying solar PV modules. This phase is critical because it lessens the computational complexity by only directing the analysis to the parts of interest and completely ignoring the background areas that are not important in the detection process. This coarse segmentation technique allows the framework to limit the search

computation applied to each pixel, resulting in an enhanced image with improved visual quality. This enhanced image is then used as the input for the second-tier segmentation, which focuses on more precise hotspot localization and classification.

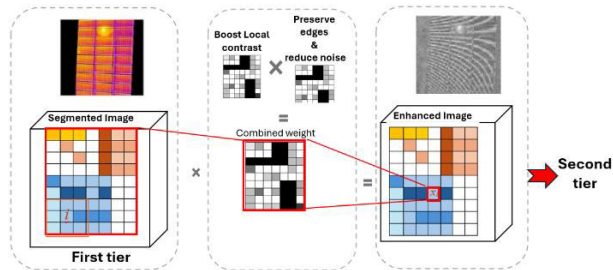


FIGURE 11. Schematic illustration of the proposed hybrid CLAHE and NLM filter applied to pixel intensity x , from segmented image at first tier output and computed as weighted sum of values for every pixel used at second tier input.

Figure 12 shows the image enhancement and evaluation process. The first step in the analysis is pre-processing the input images. Every image is reprocessed, resized, and transformed into a grayscale to improve workflow efficiency. Baseline image quality metrics, such as MSE, PSNR, and SNR, were calculated for each image in the dataset. The average improvement across the dataset was calculated to assess the effectiveness of the enhancement method.

3) SECOND TIER: FINE SEGMENTATION

The second tier of the framework is fine segmentation to achieve a more precise and detailed detection of hotspots within the solar PV modules. In this stage, advanced deep learning models, such as U-Net and ResNet, perform pixel-level segmentation within the refined regions highlighted by First tier. These models are especially effective in image segmentation tasks, as they can learn complex spatial patterns and precisely delineate the boundaries of hotspots. The U-Net architecture, with its encoder-decoder design, captures fine details. At the same time, the residual connections in ResNet play a crucial role in maintaining the integrity of features throughout the layers, ensuring that the intricate characteristics of the network are retained. In the two-tier segmentation setup, ResNet can act as the encoder (backbone) within U-Net, enhancing the initial feature extraction. Its deep layers capture intricate details and contextual information, which are essential for accurate segmentation in complex environments, like outdoor PV plants. ResNet's robust feature extraction capabilities allow the model to generalize well, even in noisy or low-resolution thermal images, making it an excellent choice for the hierarchical structure in 2TSS.

This meticulous segmentation process explores beyond the overarching anomalies recognized in first tier. It aims to extract detailed information from thermal images, highlighting aspects that may be overlooked during the initial coarse segmentation. The framework employs advanced models

Image Enhancement Algorithm (after first tier)

Begin.

Define input and output folders:

- input Folder: path to original images.
- output Folder: path to save enhanced images.

Get a list of all .jpg image files from the input folder.

Initialize arrays to store MSE, PSNR, and SNR values for each image.

For each image in the folder (using parallel loop):

- a. Read the image from the file.
- b. Convert the image to grayscale.
- c. Resize the image to 50% of its original size for faster processing.
- d. Convert the resized grayscale image to double precision format.
- e. Compute image quality metrics for the original image.
- f. Apply image enhancement.
 - for each image I in the dataset:
 - convert I to grayscale as I_{gray} .
 - resize I_{gray} to reduce computational cost.
 - convert I_{gray} to double precision format as I_{original}

% Hybrid Enhancement Pipeline:

% Step 1: Denoising using Non-Local Means (NLM)
 $I_{\text{denoised}} = \text{apply NLM filter to } I_{\text{original}} \text{ with smoothing parameter } \sigma_1 \text{ (eq.1)}$

% Step 2: Contrast Enhancement using CLAHE
 $I_{\text{enhanced}} = \text{apply CLAHE to } I_{\text{denoised}} \text{ with clip limit } c \text{ and tile grid size } t \times t \text{ (eq.2)}$

% Step 3: Evaluation (optional)
 compute MSE, PSNR, and SNR between I_{original} and I_{enhanced} (eq.3, eq.4, eq.5)

store or save I_{enhanced} for further processing or visualization
 end for

- g. Save the enhanced image to the output folder.
- h. Convert the enhanced image to double precision format.
- i. Compute image quality metrics after enhancement.
 - After processing all images:
 - Compute the average MSE, PSNR, and SNR values for both original and enhanced images.
 - Store all metrics (per image and average) onto a results table.

End.

FIGURE 12. Algorithm for implementing the proposed hybrid image enhancement after first tier segmentation.

to identify smaller or less apparent hotspots that might otherwise be overlooked. This level ensures that the framework is excellent at finding hotspots, which is essential for

keeping energy losses low to prevent solar PV panels from breaking down over time. The longevity and performance of solar energy systems are eventually increased through this technique, which facilitates more efficient monitoring and maintenance by enabling detailed hotspot detection. Figure 13 illustrates a second tier processing block diagram for analyzing solar panel images to detect hotspots.

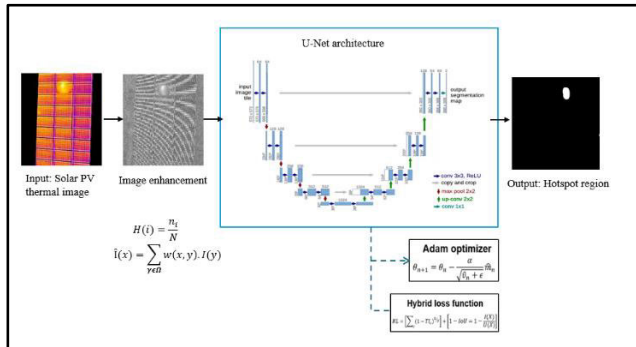


FIGURE 13. Second tier semantic segmentation is used to identify hotspots in solar panels.

The semantic segmentation methodology was employed to implement the segmentation process for both tiers in the proposed framework, as illustrated in Figure 14. The input and corresponding pixel-labeled (Region of Interest) images were loaded to initiate the process. A unique label ID was assigned to each defined class, such as background and solar panel, by implementing a label mapping function. The number of pixels per class was quantified and their frequencies plotted to analyze the class distribution and identify potential imbalances. Training, validation, and testing were the subsequent partitions of the dataset.

A suitable base network design, such as ResNet or U-Net, was chosen to create a semantic segmentation network. Class weights were calculated and used during training to solve the class imbalance. Furthermore, the final training datastore was constructed and relevant training parameters were defined. The network was trained using the training set, and its performance was assessed using the test set. Analysis was done on the evaluation outcomes, which included segmentation accuracy and quality. This entire segmentation workflow was applied to each one independently to compare the performance of the first and second segmentation phases.

D. PERFORMANCE METRICS

The evaluation of the 2TSS model was based on several widely accepted performance metrics for semantic segmentation tasks. The definition of the term used in the confusion matrix is explained in Table 4.

These metrics include:

Accuracy: The ratio of correctly classified pixels (hotspot or background) to the total number of pixels in the image. This metric provides an overall measure of the model’s performance. The best value for accuracy is 1.0 or 100%,

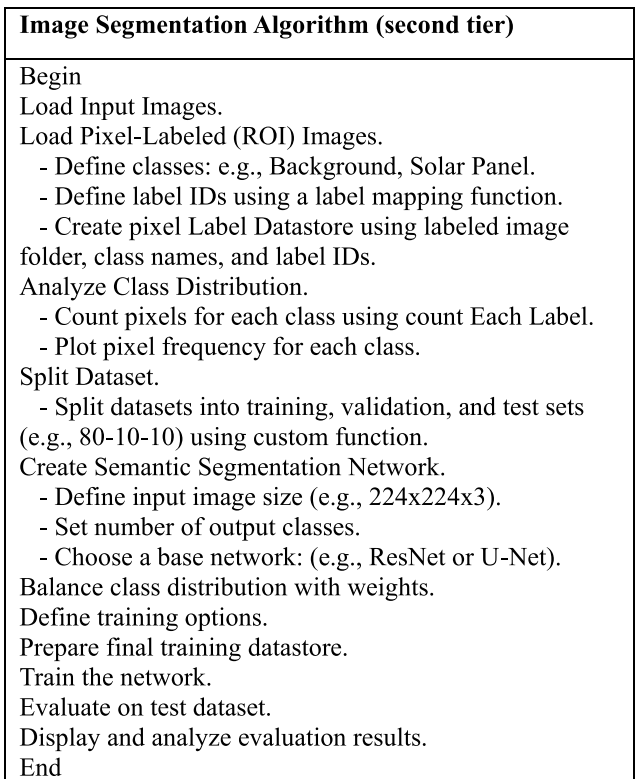


FIGURE 14. Algorithm for implementing the hotspot detection at second tier segmentation.

TABLE 4. Interpretation of the term used in confusion matrix.

| Matrix Evaluation | Interpretation |
|---------------------|--|
| True Positive (TP) | The confusion matrix shows the number of correct predictions for positive value. |
| True Negative (TN) | The confusion matrix shows the number of correct predictions for negative value. |
| False Positive (FP) | The confusion matrix shows the yes value for actual class is no. |
| False Negative (FN) | The confusion matrix shows the no value for actual class is yes. |

indicating that all determinations made by the model are correct.

$$Accuracy = \frac{TP + TN}{TP + FN + TN + FP} \tag{4}$$

Precision: The ratio of true positive hotspot pixels to the sum of true positive and false positive pixels, indicating how well the model avoids false alarms. The best value for precision is 1.0 or 100%, indicating that all positive determinations made by the model are correct with no false positives.

$$Precision = \frac{TP}{(TP + FP)} \tag{5}$$

Recall: The ratio of true positive hotspot pixels to the sum of true positive and false negative pixels, reflecting the model’s ability to detect actual hotspots. The best value for recall is 1.0 or 100%, indicating that the model successfully identifies

TABLE 5. The tuning for learning parameters for both tiers segmentation setting for semantic segmentation.

| Parameter | Settings |
|------------------------|-----------|
| Optimizer | Adam |
| Max Epoch | 80 |
| Mini Batch | 10 |
| Learning Rate | 10 |
| Learn Rate Drop Factor | 0.3 |
| Threshold | 10^{-4} |

all actual positive instances with no false negatives.

$$Recall = \frac{TP}{(TP + FN)} \quad (6)$$

Intersection over Union (IoU): A metric used to assess the overlap between the predicted hotspot regions and the ground truth annotations. IoU is especially useful in segmentation tasks for evaluating the accuracy of the predicted region boundaries. The best value for IoU is 1.0 or 100%, indicating that the predicted regions perfectly overlap with the ground truth regions, with no misalignment or errors.

$$IoU = \frac{TP}{(TP + FP + FN)} \quad (7)$$

These metrics were calculated for both the coarse and fine segmentation stages of the 2TSS framework to assess the effectiveness of each tier independently, as well as the overall performance of the combined model.

IV. RESULTS

This section provides an in-depth evaluation of the effectiveness of semantic segmentation for solar PV panels and hotspots. Table 5 outlines the tuned hyperparameters used to ensure optimal model performance by training the semantic segmentation models in both tiers of the hotspot detection framework.

A. PERFORMANCE OF FIRST-TIER SEGMENTATION

As mentioned, the first tier of the segmentation phase was applied to segregate the solar panel from the background. Meanwhile, the second segmentation was performed to discriminate between the segregated solar panel and the hotspot region.

Figure 15 presents the outcomes of the first tier segmentation using three different deep learning architectures, namely U-Net, ResNet 18, and ResNet 50. The segmented images from first tier segmentation were divided into two main clusters to represent the solar panel and the background.

Firstly, Figure 15(a) shows the U-Net model showing relatively accurate segmentation but with minor misclassifications along the panel edges, indicating potential sensitivity to boundary noise variations. Next, Figure 15(b) demonstrates ResNet 18 improved edge sharpness compared to U-Net, especially in separating tightly clustered panel units.

However, some background noise persists around the outer boundaries, which may suggest limitations in in-depth representation due to the shallower architecture.

Finally, Figure 15(c) displays the result of ResNet 50, which yields the most refined and clean segmentation. The solar panel regions are more clearly delineated with minimal background interference. In contrast to the previous two models, ResNet 50 shows improved precision, likely due to its deeper network structure that allows for more robust feature extraction.

Overall, these results highlight the increasing segmentation quality from U-Net to ResNet 50, indicating that deeper models contribute significantly to more accurate and reliable segmentation in solar panel imagery.

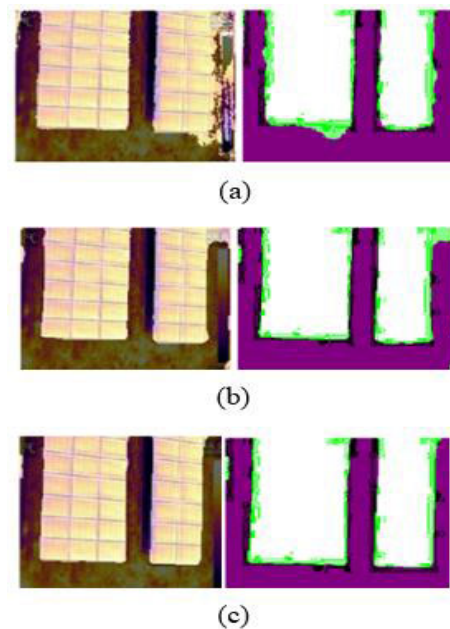


FIGURE 15. Example of segmented solar panel (ROI) and background in thermal images using (a) U-Net (minor classification) (b) ResNet 18 (improved edge with noise) (c) ResNet 50 (most refined) at first tier segmentation method.

Table 6 illustrates the initial segmentation results for classifying solar PV and background. This result compares the performance of three semantic segmentation models between U-Net, ResNet 18, and ResNet 50. ResNet 50 leads with a mean accuracy of 0.9833 and a mean IoU of 0.9641, making it the top performer for general segmentation accuracy and overlapping with ground truth. ResNet 18 follows closely with a mean accuracy of 0.9755 and an IoU of 0.9569, and it records the highest precision of 0.9975 and recall of 0.9880, indicating its strength in minimizing false positives and false negatives. Although commonly used in many segmentation tasks, U-Net shows the lowest performance across all metrics in this scenario, with a mean accuracy of 0.9503 and IoU of 0.9154.

ResNet 50 has the most reliable segmentation performance, making it perfect for an application where maximum

TABLE 6. The first segmentation result.

| Semantic Model | Mean accuracy | Mean IoU | Precision | Recall | Execution Time (min) |
|------------------|---------------|---------------|---------------|---------------|----------------------|
| U-Net | 0.9503 | 0.9154 | 0.9828 | 0.9497 | 22 |
| ResNet 18 | 0.9755 | 0.9569 | 0.9975 | 0.9880 | 12 |
| ResNet 50 | 0.9833 | 0.9641 | 0.9687 | 0.9879 | 23 |

overall accuracy and IoU are essential. ResNet 18 is more suitable for applications that value detection reliability due to its improved precision and recall. ResNet-based models are more suited for thermal image segmentation associated with solar PV research since U-Net is reliable for general segmentation tasks but performs very poorly in this context.

The computationally most efficient model, ResNet 18, completed the task in 12 minutes, followed by U-Net at 22 minutes and ResNet 50 at 23 minutes. When balancing processing speed and segmentation effectiveness, ResNet 18 is the best choice, especially in situations with limited resources or time.

B. PERFORMANCE OF IMAGE ENHANCEMENT

This part evaluates the effectiveness of the proposed image enhancement method by comparing the original and improved images both visually and quantitatively. Enhancing image quality, lowering noise, and emphasizing important structural components are the main goals of the enhancement method, particularly when it comes to low-resolution thermal images used for PV system studies. Basic image quality measurements, including Mean Squared Error (MSE), Peak Signal-to-Noise Ratio (PSNR), and Signal-to-Noise Ratio (SNR), are employed to evaluate the efficacy of the enhancement technique.

Figure 16 shows a side-by-side visual comparison of the original and enhanced images after the proposed CLAHE and NLM hybrid enhancement method. Visually, the improved photos show better contrast, less noise, and more distinct structural patterns, particularly in regions with low contrast. The repetitive textures in the thermal patterns become more distinguishable, crucial for improving downstream analysis such as segmentation or defect detection in PV modules.

Quantitative results in Table 7 further support the visual improvement. The MSE value increased slightly from 0 to 2.297×10^{-4} , which is expected after enhancement due to added contrast adjustments. The PSNR, which reflects overall image clarity, decreased from “infinite” (due to MSE being zero in the original) to 36.469, which still indicates high image quality. The SNR decreased from 93.402 to 29.861, indicating that although contrast amplification introduced noise, the image enhancement process successfully preserved critical image features.

Overall, visual and metric-based evaluations demonstrate that the enhancement improves image clarity and structural

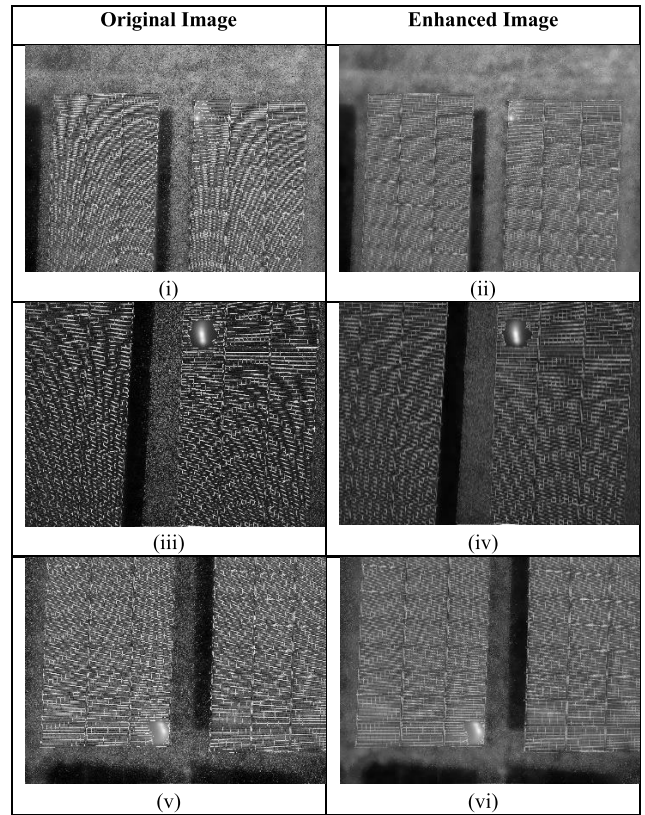


FIGURE 16. Comparison between original (i),(iii),(v) and enhanced image (ii),(iv),(vi) using proposed hybrid CLAHE and NLM method.

TABLE 7. Quantitative comparison of image quality metrics between the original and enhanced images.

| Parameter | Original Image | Enhance Image |
|-----------|----------------|------------------------|
| MSE | 0 | 2.297×10^{-4} |
| PSNR | Inf | 36.469 |
| SNR | 93.402 | 29.861 |

visibility. This makes the enhanced images more suitable for subsequent analysis, such as segmentation or classification tasks.

C. PERFORMANCE OF SECOND TIER SEGMENTATION

As previously noted, the second tier segmentation further refines the output from the first tier thermal image segmentation by clustering the image into solar PV panel and hotspot regions. Figure 17 suggests that ResNet 50 delivers the best segmentation results, showing refined and well-preserved details of the region of interest. ResNet 18 follows with slightly less precision but still offers a reasonable segmentation outcome. U-Net appears to perform the weakest in this comparison, with fewer distinct boundaries and details. This finding would imply that ResNet 50’s more profound architecture is better suited to capturing the complexity of the area. Furthermore, the shallower ResNet 18 network performed U-Net, which may not have been optimally suited for this specific application.

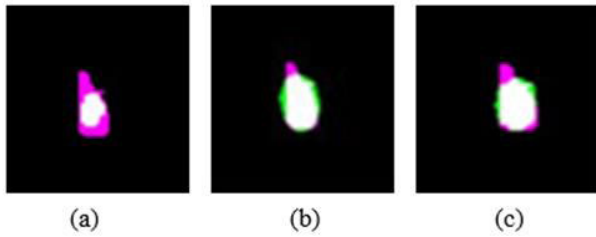


FIGURE 17. Sample of result for the second-tier segmentation for (a) U-Net (b) ResNet 18 (c) ResNet 50 architecture.

TABLE 8. The second segmentation result (before enhancement).

| Semantic Model | Mean accuracy | Mean IoU | Precision | Recall | Execution Time (min) |
|----------------|---------------|----------|-----------|--------|----------------------|
| U-Net | 0.6478 | 0.6383 | 0.9968 | 0.9990 | 22 |
| ResNet 18 | 0.7245 | 0.5557 | 0.9975 | 0.9879 | 12 |
| ResNet 50 | 0.8556 | 0.7698 | 0.9986 | 0.9985 | 24 |

TABLE 9. The second segmentation result (after enhancement).

| Semantic Model | Mean accuracy | Mean IoU | Precision | Recall | Execution Time (min) |
|----------------|---------------|----------|-----------|--------|----------------------|
| U-Net | 0.6450 | 0.6370 | 0.9968 | 0.9998 | 22 |
| ResNet 18 | 0.8810 | 0.7861 | 0.9989 | 0.9983 | 12 |
| ResNet 50 | 0.8782 | 0.7895 | 0.9989 | 0.9986 | 24 |

Tables 8 and 9 summarize the second-tier segmentation results before and after applying the proposed enhancement method. This evaluation involves three semantic segmentation models. After enhancement, ResNet 50 was performed, increasing mean accuracy from 0.8556 to 0.8782 and mean IoU from 0.7698 to 0.7895. These findings demonstrate how consistently and successfully it can recognize intricate thermal patterns in PV images. With a mean accuracy increase from 0.7245 to 0.8810 and a mean IoU increase from 0.5557 to 0.7861, ResNet 18 also demonstrated a significant improvement, thus establishing it as a high-performing model with enhanced feature recognition. In contrast, U-Net records a slight drop in both metrics, suggesting that its simpler architecture may not fully benefit from the enhanced visual features.

ResNet 50 is still the most dependable model since it consistently provides high segmentation quality, particularly when accuracy and detail retention are crucial. Despite having a little lower accuracy than ResNet 50, ResNet 18 is far more efficient in processing time, which makes it ideal for real-world applications that demand quicker results. U-Net, while commonly applied in segmentation tasks, demonstrated the lowest performance in this context across both stages.

In relation to processing speed, ResNet 18 consistently completes segmentation in 12 minutes, followed by U-Net

TABLE 10. State-of-the-art performance comparison.

| Author / Year | Method Used | Accuracy (%) | Improvement (%) |
|----------------------------|---|--|-----------------|
| F. Wang et al., 2023. [19] | Improved Mask R-CNN. | 75.04 | 13.4 |
| L.Chen et al., 2023.[57] | Improved FCN Network. | 98.00 | No information |
| Y.Lei et al.,2024. [58] | Deeplabv3+ semantic segmentation (MobileNetV2 backbone and CBAM attention). | 95.01 | 2.61 |
| This Study, 2025. | CLAHE, NLM and ResNet + Semantic segmentation. | 98.33 (First segmentation). 87.82 (Second segmentation). | 2.62 |

in 22 minutes and ResNet 50 in 24 minutes. While ResNet 50 remains the greatest option when segmentation precision is the top priority, ResNet 18 offers the best balance when segmentation accuracy and processing time are considered, especially when time is essential.

Finally, the suggested image enhancement method using CLAHE and Non-Local Means improves image quality and enables better segmentation results. The results indicate that enhanced images enable deep-learning models such as ResNet 18 and ResNet 50 to get superior accuracy and feature localization. ResNet 50 is the best segmentation model among all those tested, while ResNet 18 strikes a respectable balance between computational efficiency and accuracy. These outcomes demonstrate the effectiveness of the improvement framework in facilitating accurate and efficient hotspot identification in PV systems.

V. LIMITATION AND DISCUSSION

Hotspots come in various complex shapes, patterns, and morphologies, which present significant challenges for manual annotation of regions of interest. This process is prone to human error and subjective biases, resulting in inaccurate annotations. Such inaccuracies negatively impact the training and performance of segmentation models, ultimately leading to lower IoU values.

Table 10 compares recent PV hotspot segmentation and detection methods, highlighting performance improvements and ongoing limitations. Early edge-guided models improved segmentation accuracy from 61.64% to 75.04% but suffered from poor edge extraction and high missed detection rates [19]. Later approaches using semantic segmentation with migration networks achieved up to 98% accuracy yet struggled with precise hotspot localization [56]. A more advanced technique combined improved Deeplabv3+ and YOLOv5 architectures, attaining 95.01% segmentation accuracy and high detection precision, though small hotspot detection remained limited [57] In comparison, this study

achieved 98.33% and 87.82% accuracy across two segmentation stages but was affected by annotation inconsistency and hotspot complexity.

Compared to previous studies, this work is conducted in a more practical and challenging setting, using real thermal images of PV panels with minimal manual pre-processing. Although the segmentation performance may appear slightly lower in ideal conditions, the proposed method remains robust when applied to realistic environments where hotspot shapes are highly irregular, and annotations are inconsistent. The technique successfully manages hotspot appearance variability, showcasing deep learning's capacity to generalize well in challenging thermal imaging conditions.

The study concludes that the suggested hybrid enhancement and deep learning framework produce reliable and valid results, even if hotspot segmentation is inherently complex. These results are appropriate for PV inspection systems in the real world, where inconsistent hotspot morphology and data quality are still significant challenges. The approach demonstrates strong potential for further development into a scalable, field-deployable diagnostic solution.

VI. CONCLUSION

This research introduced a novel Two-Tier Semantic Segmentation (2TSS) framework to address the limitations of current hotspot segmentation methods in solar PV systems. The experimental results demonstrated that ResNet 50 consistently achieved the highest accuracy and IoU for the first and second-tier segmentation processes. The first-tier segmentation attained an accuracy of 98.33% and an IoU of 0.9641, while the second-tier segmentation recorded an accuracy of 85.56% and an IoU of 0.76981. The findings validate the effectiveness of the 2TSS framework, demonstrating its advantages over traditional models across various performance metrics. The 2TSS architecture demonstrates significant adaptability and generalizability. It facilitates accurate segmentation even in difficult settings, such as low-resolution thermal images, noise interference, and variable environmental parameters. The lower accuracy observed in the second segmentation tier can be attributed to the intricacy of the pores' shape, pattern, and morphology. Future initiatives should refine the framework to more efficiently handle low-resolution images by applying advanced techniques such as image upscaling, model pruning, and quantization. By enhancing the accuracy and efficacy of hotspot detection, the 2TSS framework offers a dependable solution for preventive maintenance and real-time diagnostics in solar PV systems. This framework contributes to the broader goal of advancing renewable energy technology, promoting sustainability, and increasing the efficiency of solar power generation.

ACKNOWLEDGMENT

The authors wish to thank Centre for Electrical Engineering, Universiti Teknologi MARA, Cawangan Pulau Pinang, for

administrative and facilities supports. Special thanks to Universiti Malaysia Pahang, Pekan, Malaysia.

REFERENCES

- [1] A. O. M. Maka and J. M. Alabid, "Solar energy technology and its roles in sustainable development," *Clean Energy*, vol. 6, no. 3, pp. 476–483, Jun. 2022, doi: [10.1093/ce/zkac023](https://doi.org/10.1093/ce/zkac023).
- [2] M. Dhimish, M. Theristis, and V. D' Alessandro, "Photovoltaic hotspots: A mitigation technique and its thermal cycle," *Optik*, vol. 300, Apr. 2024, Art. no. 171627, doi: [10.1016/j.ijleo.2024.171627](https://doi.org/10.1016/j.ijleo.2024.171627).
- [3] A. Fatani and A. AlAhdal, "Inspections and detection system for hotspots in photovoltaic farms using UAV," in *Proc. Int. Conf. Eng. Emerg. Technol. (ICEET)*, Oct. 2022, pp. 1–6, doi: [10.1109/ICEET56468.2022.10007113](https://doi.org/10.1109/ICEET56468.2022.10007113).
- [4] A. Oulefki, Y. Himeur, T. Trongtirakul, K. Amara, S. Agaian, S. Benbelkacem, M. A. Guerroudji, M. Zemmouri, S. Ferhat, N. Zenati, S. Atalla, and W. Mansoor, "Detection and analysis of deteriorated areas in solar PV modules using unsupervised sensing algorithms and 3D augmented reality," *Heliyon*, vol. 10, no. 6, Mar. 2024, Art. no. e27973, doi: [10.1016/j.heliyon.2024.e27973](https://doi.org/10.1016/j.heliyon.2024.e27973).
- [5] H. Ling, M. Liu, and Y. Fang, "Deep edge-based fault detection for solar panels," *Sensors*, vol. 24, no. 16, p. 5348, Aug. 2024, doi: [10.3390/s24165348](https://doi.org/10.3390/s24165348).
- [6] E. H. Sepúlveda-Oviedo, L. Travé-Massuyès, A. Subias, M. Pavlov, and C. Alonso, "Fault diagnosis of photovoltaic systems using artificial intelligence: A bibliometric approach," *Heliyon*, vol. 9, no. 11, Nov. 2023, Art. no. e21491, doi: [10.1016/j.heliyon.2023.e21491](https://doi.org/10.1016/j.heliyon.2023.e21491).
- [7] M. E. Rayed, S. M. S. Islam, S. I. Niha, J. R. Jim, M. M. Kabir, and M. F. Mridha, "Deep learning for medical image segmentation: State-of-the-art advancements and challenges," *Informat. Med. Unlocked*, vol. 47, Jan. 2024, Art. no. 101504, doi: [10.1016/j.imu.2024.101504](https://doi.org/10.1016/j.imu.2024.101504).
- [8] M. Salvi, U. R. Acharya, F. Molinari, and K. M. Meiburger, "The impact of pre- and post-image processing techniques on deep learning frameworks: A comprehensive review for digital pathology image analysis," *Comput. Biol. Med.*, vol. 128, Jan. 2021, Art. no. 104129, doi: [10.1016/j.cmpbiomed.2020.104129](https://doi.org/10.1016/j.cmpbiomed.2020.104129).
- [9] M. Aghaei, A. Fairbrother, A. Gok, S. Ahmad, S. Kazim, K. Lobato, G. Oreski, A. Reinders, J. Schmitz, M. Theelen, P. Yilmaz, and J. Kettle, "Review of degradation and failure phenomena in photovoltaic modules," *Renew. Sustain. Energy Rev.*, vol. 159, May 2022, Art. no. 112160, doi: [10.1016/j.rser.2022.112160](https://doi.org/10.1016/j.rser.2022.112160).
- [10] A. Alhabib, K. Itako, and T. Kudoh, "Development of real-time hotspot detection system utilizing artificial intelligence in PV generation system," *J. Adv. Sci.*, vol. 32, p. 32103, May 2020, doi: [10.2978/jasas.32103](https://doi.org/10.2978/jasas.32103).
- [11] M. Z. A. Hamid, K. Daud, Z. H. C. Soh, M. K. Osman, I. S. Isa, and N. H. Ishak, "Review of deep learning-based hotspot detection in solar photovoltaic arrays," in *Proc. IEEE 4th Int. Conf. Power Eng. Appl. (ICPEA)*, Mar. 2024, pp. 332–337, doi: [10.1109/ICPEA60617.2024.10498989](https://doi.org/10.1109/ICPEA60617.2024.10498989).
- [12] N. H. Binti Ishak, I. Sazanita Binti Isa, M. K. Bin Osman, K. Daud, and M. S. Bin Jadin, "Hotspot detection of solar photovoltaic system: A perspective from image processing," in *Proc. IEEE 3rd Int. Conf. Power Eng. Appl. (ICPEA)*, Mar. 2023, pp. 263–267, doi: [10.1109/ICPEA56918.2023.10093148](https://doi.org/10.1109/ICPEA56918.2023.10093148).
- [13] H. Açıkgöz, D. Korkmaz, and Ç. Dandil, "Classification of hotspots in photovoltaic modules with deep learning methods," *Turkish J. Sci. Technol.*, vol. 17, no. 2, pp. 211–221, Sep. 2022, doi: [10.55525/tjst.1158854](https://doi.org/10.55525/tjst.1158854).
- [14] S. Abdulateef and M. Salman, "A comprehensive review of image segmentation techniques," *Iraqi J. Electr. Electron. Eng.*, vol. 17, no. 2, pp. 166–175, Dec. 2021, doi: [10.37917/ijeee.17.2.18](https://doi.org/10.37917/ijeee.17.2.18).
- [15] Y. Su, F. Tao, J. Jin, and C. Zhang, "Automated overheated region object detection of photovoltaic module with thermography image," *IEEE J. Photovolt.*, vol. 11, no. 2, pp. 535–544, Mar. 2021, doi: [10.1109/JPHOTOV.2020.3045680](https://doi.org/10.1109/JPHOTOV.2020.3045680).
- [16] Y. Chen, Y. Lin, T. Gai, Y. Su, Y. Wei, and D. Z. Pan, "Semisupervised hotspot detection with self-paced multitask learning," *IEEE Trans. Comput.-Aided Design Integr. Circuits Syst.*, vol. 39, no. 7, pp. 1511–1523, Jul. 2020, doi: [10.1109/TCAD.2019.2912948](https://doi.org/10.1109/TCAD.2019.2912948).
- [17] Z. Guo, Z. Zhuang, H. Tan, Z. Liu, P. Li, Z. Lin, W.-L. Shang, H. Zhang, and J. Yan, "Accurate and generalizable photovoltaic panel segmentation using deep learning for imbalanced datasets," *Renew. Energy*, vol. 219, Dec. 2023, Art. no. 119471.

- [18] Y. Wang, Y. Shen, C. Li, K. Zhang, and H. Wei, "Hotspot detection of photovoltaic modules in infrared thermal image based on saliency analysis," in *Proc. 34th Chin. Control Decis. Conf. (CCDC)*, Aug. 2022, pp. 1479–1484, doi: [10.1109/CCDC55256.2022.10033497](https://doi.org/10.1109/CCDC55256.2022.10033497).
- [19] F. Wang, Z. Wang, Z. Chen, D. Zhu, X. Gong, and W. Cong, "An edge-guided deep learning solar panel hotspot thermal image segmentation algorithm," *Appl. Sci.*, vol. 13, no. 19, p. 11031, Oct. 2023, doi: [10.3390/app131911031](https://doi.org/10.3390/app131911031).
- [20] M. Z. A. Hamid, K. Daud, Z. H. C. Soh, M. K. Osman, I. S. Isa, and M. S. Jadin, "Deep learning-driven thermal imaging hotspot detection in solar photovoltaic arrays using YOLOv10," *ESTEEM Academic J.*, vol. 20, pp. 77–90, Sep. 2024, doi: [10.24191/esteem.v20iseptember.1861.g1773](https://doi.org/10.24191/esteem.v20iseptember.1861.g1773).
- [21] Y. Jia, G. Chen, and L. Zhao, "Defect detection of photovoltaic modules based on improved VarifocalNet," *Sci. Rep.*, vol. 14, no. 1, pp. 1–14, Jul. 2024, doi: [10.1038/s41598-024-66234-3](https://doi.org/10.1038/s41598-024-66234-3).
- [22] U. Hijjawi, S. Lakshminarayana, T. Xu, G. Piero Malfense Fierro, and M. Rahman, "A review of automated solar photovoltaic defect detection systems: Approaches, challenges, and future orientations," *Sol. Energy*, vol. 266, Dec. 2023, Art. no. 112186, doi: [10.1016/j.solener.2023.112186](https://doi.org/10.1016/j.solener.2023.112186).
- [23] H. Li, S. Wang, S. Li, H. Wang, S. Wen, and F. Li, "Thermal infrared-image-enhancement algorithm based on multi-scale guided filtering," *Fire*, vol. 7, no. 6, p. 192, Jun. 2024, doi: [10.3390/fire7060192](https://doi.org/10.3390/fire7060192).
- [24] R. A. Haleot, Z. M. Abood, and G. Karam, "Thermal image enhancement algorithm based on adaptive fusion technique of multi color space," *Int. J. Eng. Res. Adv. Technol.*, vol. 6, no. 9, pp. 10–15, 2020, doi: [10.31695/ijerat.2020.3637](https://doi.org/10.31695/ijerat.2020.3637).
- [25] U. Kuran and E. C. Kuran, "Parameter selection for CLAHE using multi-objective cuckoo search algorithm for image contrast enhancement," *Intell. Syst. Appl.*, vol. 12, Nov. 2021, Art. no. 200051, doi: [10.1016/j.iswa.2021.200051](https://doi.org/10.1016/j.iswa.2021.200051).
- [26] V. V. Naik and S. Gharge, "Satellite image resolution enhancement using DTCWT and DTCWT based fusion," in *Proc. Int. Conf. Adv. Comput., Commun. Informat. (ICACCI)*, Sep. 2016, pp. 1957–1962, doi: [10.1109/ICACCI.2016.7732338](https://doi.org/10.1109/ICACCI.2016.7732338).
- [27] X. Liu, T. Do, and C. Nguyen, "Medical images enhancement by integrating CLAHE with wavelet transform and non-local means denoising," *Academic J. Comput. Inf. Sci.*, vol. 7, no. 1, pp. 52–58, 2024, doi: [10.25236/ajcis.2024.070108](https://doi.org/10.25236/ajcis.2024.070108).
- [28] H. Zhang, Z. Jiang, X. Yao, and S. Chen, "An improved semantic segmentation network for ultra-high resolution remote sensing images based on DeepLabV3+," in *Proc. 3rd Int. Conf. Electron. Inf. Eng. Comput. Sci. (EIECS)*, Sep. 2023, pp. 815–820, doi: [10.1109/EIECS59936.2023.10435470](https://doi.org/10.1109/EIECS59936.2023.10435470).
- [29] Z. Li, W. Liu, G. Wu, and S. Yang, "Semantic segmentation of unmanned aerial vehicle image based on ResNet-UNet," in *Proc. 8th Int. Conf. Informat. Biomed. Sci. (ICIBMS)*, Nov. 2023, pp. 295–299, doi: [10.1109/ICIBMS60103.2023.10347663](https://doi.org/10.1109/ICIBMS60103.2023.10347663).
- [30] S. Cai, Y. Tian, H. Lui, H. Zeng, Y. Wu, and G. Chen, "Dense-UNet: A novel multiphoton in vivo cellular image segmentation model based on a convolutional neural network," *Quant. Imag. Med. Surgery*, vol. 10, no. 6, pp. 1275–1285, Jun. 2020, doi: [10.21037/qims-19-1090](https://doi.org/10.21037/qims-19-1090).
- [31] N. Siddique, S. Paheding, C. P. Elkin, and V. Devabhaktuni, "U-net and its variants for medical image segmentation: A review of theory and applications," *IEEE Access*, vol. 9, pp. 82031–82057, 2021, doi: [10.1109/ACCESS.2021.3086020](https://doi.org/10.1109/ACCESS.2021.3086020).
- [32] S. Deitsch, C. Buerhop-Lutz, E. Sovetkin, A. Steland, A. Maier, F. Gallwitz, and C. Riess, "Segmentation of photovoltaic module cells in uncalibrated electroluminescence images," *Mach. Vis. Appl.*, vol. 32, no. 4, pp. 1–23, Jul. 2021, doi: [10.1007/s00138-021-01191-9](https://doi.org/10.1007/s00138-021-01191-9).
- [33] J. J. Vasanth, S. N. Venkatesh, V. Sugumaran, and V. S. Mahamuni, "Enhancing photovoltaic module fault diagnosis with unmanned aerial vehicles and deep learning-based image analysis," *Int. J. Photoenergy*, vol. 2023, pp. 1–17, Jul. 2023, doi: [10.1155/2023/8665729](https://doi.org/10.1155/2023/8665729).
- [34] J. Li, R. Gong, and G. Wang, "Enhancing fitness action recognition with ResNet-TransFit: Integrating IoT and deep learning techniques for real-time monitoring," *Alexandria Eng. J.*, vol. 109, pp. 89–101, Dec. 2024, doi: [10.1016/j.aej.2024.07.068](https://doi.org/10.1016/j.aej.2024.07.068).
- [35] A. B. Amjoud and M. Amrouh, "Object detection using deep learning, CNNs and vision transformers: A review," *IEEE Access*, vol. 11, pp. 35479–35516, 2023, doi: [10.1109/ACCESS.2023.3266093](https://doi.org/10.1109/ACCESS.2023.3266093).
- [36] I. Qureshi, J. Yan, Q. Abbas, K. Shaheed, A. B. Riaz, A. Wahid, M. W. J. Khan, and P. Szczuko, "Medical image segmentation using deep semantic-based methods: A review of techniques, applications and emerging trends," *Inf. Fusion*, vol. 90, pp. 316–352, Feb. 2023, doi: [10.1016/j.inffus.2022.09.031](https://doi.org/10.1016/j.inffus.2022.09.031).
- [37] D. Liu, D. Zhang, L. Wang, and J. Wang, "Semantic segmentation of autonomous driving scenes based on multi-scale adaptive attention mechanism," *Frontiers Neurosci.*, vol. 17, pp. 1–12, Oct. 2023, doi: [10.3389/fnins.2023.1291674](https://doi.org/10.3389/fnins.2023.1291674).
- [38] W. M. Elmessery, D. V. Maklakov, T. M. El-Messery, D. A. Baranenko, J. Gutiérrez, M. Y. Shams, T. A. El-Hafeez, S. Elsayed, S. K. Alhag, F. S. Moghann, M. A. Mulyukin, Y. Y. Petrova, and A. E. Elwakeel, "Semantic segmentation of microbial alterations based on SegFormer," *Frontiers Plant Sci.*, vol. 15, pp. 1–20, Jun. 2024, doi: [10.3389/fpls.2024.1352935](https://doi.org/10.3389/fpls.2024.1352935).
- [39] R. A. M. Rudro, K. Nur, M. F. A. A. Sohan, M. F. Mridha, S. Alfarhood, M. Safran, and K. Kanagarathinam, "SPF-net: Solar panel fault detection using U-net based deep learning image classification," *Energy Rep.*, vol. 12, pp. 1580–1594, Dec. 2024, doi: [10.1016/j.egy.2024.07.044](https://doi.org/10.1016/j.egy.2024.07.044).
- [40] Z. Wang, J. Wang, K. Yang, L. Wang, F. Su, and X. Chen, "Semantic segmentation of high-resolution remote sensing images based on a class feature attention mechanism fused with Deeplabv3+," *Comput. Geosci.*, vol. 158, Jan. 2022, Art. no. 104969, doi: [10.1016/j.cageo.2021.104969](https://doi.org/10.1016/j.cageo.2021.104969).
- [41] T. H. Rafi, R. Mahjabin, E. Ghosh, Y.-W. Ko, and J.-G. Lee, "Domain generalization for semantic segmentation: A survey," *Artif. Intell. Rev.*, vol. 57, no. 9, pp. 1–30, Aug. 2024, doi: [10.1007/s10462-024-10817-z](https://doi.org/10.1007/s10462-024-10817-z).
- [42] S. Kovalskyi and V. Koval, "Comparison of image processing techniques for defect detection," in *Proc. CEUR Workshop*, vol. 3716, 2024, pp. 158–167.
- [43] I. Segovia Ramírez, F. P. García Márquez, and J. Parra Chaparro, "Convolutional neural networks and Internet of Things for fault detection by aerial monitoring of photovoltaic solar plants," *Measurement*, vol. 234, Jul. 2024, Art. no. 114861, doi: [10.1016/j.measurement.2024.114861](https://doi.org/10.1016/j.measurement.2024.114861).
- [44] T. Tajwar, O. H. Mobin, F. R. Khan, S. F. Hossain, M. Islam, and M. M. Rahman, "Infrared thermography based hotspot detection of photovoltaic module using YOLO," in *Proc. IEEE 12th Energy Convers. Congr. Expo.-Asia (ECCE-Asia)*, May 2021, pp. 1542–1547, doi: [10.1109/ECCE-Asia49820.2021.9478998](https://doi.org/10.1109/ECCE-Asia49820.2021.9478998).
- [45] M. I. Ameerudin, M. H. Jamaluddin, A. Z. Shukor, L. A. H. Kamaruzaman, and S. Mohamad, "Towards efficient solar panel inspection: A YOLO-based method for hotspot detection," in *Proc. IEEE 14th Symp. Comput. Appl. Ind. Electron. (ISCAIE)*, May 2024, pp. 367–372, doi: [10.1109/ISCAIE61308.2024.10576312](https://doi.org/10.1109/ISCAIE61308.2024.10576312).
- [46] T. Sun, H. Xing, S. Cao, Y. Zhang, S. Fan, and P. Liu, "A novel detection method for hot spots of photovoltaic (PV) panels using improved anchors and prediction heads of YOLOv5 network," *Energy Rep.*, vol. 8, pp. 1219–1229, Nov. 2022, doi: [10.1016/j.egy.2022.08.130](https://doi.org/10.1016/j.egy.2022.08.130).
- [47] T. Özer and Ö. Türkmen, "An approach based on deep learning methods to detect the condition of solar panels in solar power plants," *Comput. Electr. Eng.*, vol. 116, May 2024, Art. no. 109143, doi: [10.1016/j.compeleceng.2024.109143](https://doi.org/10.1016/j.compeleceng.2024.109143).
- [48] Q. Zheng, J. Ma, M. Liu, Y. Liu, Y. Li, and G. Shi, "Lightweight hotspot fault detection model of photovoltaic panels in UAV remote-sensing image," *Sensors*, vol. 22, no. 12, p. 4617, 2022.
- [49] Z. Xu, Y. Shen, K. Zhang, and H. Wei, "A segmentation method for PV modules in infrared thermography images," in *Proc. 13th IEEE PES Asia-Pacific Power Energy Eng. Conf. (APPEEC)*, Nov. 2021, pp. 1–5, doi: [10.1109/APPEEC50844.2021.9687630](https://doi.org/10.1109/APPEEC50844.2021.9687630).
- [50] M. U. Ali, A. Zafar, W. Ahmed, M. Aslam, and S. H. Kim, "Enhancing photovoltaic reliability: A global and local feature selection approach with improved Harris hawks optimization for efficient hotspot detection using infrared imaging," *Int. J. Energy Res.*, vol. 2024, no. 1, Jan. 2024, Art. no. 5586605, doi: [10.1155/2024/5586605](https://doi.org/10.1155/2024/5586605).
- [51] C. Cheng, M. Liu, H. Yi, J. Wang, and H. Chen, "Tendency-aided data-driven method for hot spot detection in photovoltaic systems," *IEEE J. Emerg. Sel. Topics Ind. Electron.*, vol. 3, no. 4, pp. 901–910, Oct. 2022, doi: [10.1109/JESTIE.2022.3140648](https://doi.org/10.1109/JESTIE.2022.3140648).
- [52] A. N. N. Afifah, Indrabayu, A. Suyuti, and Syafaruddin, "Hotspot detection in photovoltaic module using Otsu thresholding method," in *Proc. IEEE Int. Conf. Commun., Netw. Satell. (Commnetsat)*, Dec. 2020, pp. 408–412.

- [53] A. Greco, C. Pironti, A. Saggese, M. Vento, and V. Vigilante, "A deep learning based approach for detecting panels in photovoltaic plants," in *Proc. 3rd Int. Conf. Appl. Intell. Syst.*, Jan. 2020, pp. 1–7, doi: [10.1145/3378184.3378185](https://doi.org/10.1145/3378184.3378185).
- [54] D. P. Winston, M. S. Murugan, R. M. Elavarasan, R. Pugazhendhi, O. J. Singh, P. Murugesan, M. Gurudhachanamoorthy, and E. Hossain, "Solar PV's micro crack and hotspots detection technique using NN and SVM," *IEEE Access*, vol. 9, pp. 127259–127269, 2021.
- [55] R. Zhu, D. Guo, M. S. Wong, Z. Qian, M. Chen, B. Yang, B. Chen, H. Zhang, L. You, J. Heo, and J. Yan, "Deep solar PV refiner: A detail-oriented deep learning network for refined segmentation of photovoltaic areas from satellite imagery," *Int. J. Appl. Earth Observ. Geoinf.*, vol. 116, Feb. 2023, Art. no. 103134, doi: [10.1016/j.jag.2022.103134](https://doi.org/10.1016/j.jag.2022.103134).
- [56] L. Chen, B. Liu, K. Sun, and J. Zhao, "A hot spot detection method of photovoltaic module based on image semantic segmentation," in *Proc. IEEE 6th Int. Electr. Energy Conf. (CIEEC)*, May 2023, pp. 837–841, doi: [10.1109/CIEEC58067.2023.10167018](https://doi.org/10.1109/CIEEC58067.2023.10167018).
- [57] Y. Lei, X. Wang, A. An, and H. Guan, "Deepplab-YOLO: A method for detecting hot-spot defects in infrared image PV panels by combining segmentation and detection," *J. Real-Time Image Process.*, vol. 21, no. 2, p. 52, Apr. 2024, doi: [10.1007/s11554-024-01415-x](https://doi.org/10.1007/s11554-024-01415-x).



NURUL HUDA ISHAK received the bachelor's degree in electrical engineering from the Universiti Teknologi MARA (UiTM), Malaysia, in 2007, and the M.Sc. degree from the Universiti Sains Malaysia, Malaysia, in 2009. In 2007, she joined UiTM, Penang Campus, Malaysia, as a Young Lecturer and has been promoted as a Senior Lecturer with the School of Electrical Engineering, College of Engineering, UiTM, Penang Branch, in 2011. She is currently a Senior Lecturer with the

Faculty of Electrical Engineering, UiTM. Her research and teaching interests include theory and application of power systems, renewable energy, image processing, and artificial intelligence-related research.



IZA SAZANITA ISA (Member, IEEE) received the bachelor's degree in electrical engineering from the Universiti Teknologi MARA (UiTM), Penang Campus, Malaysia, in 2004, the M.Sc. degree from the Universiti Sains Malaysia (USM), Malaysia, in 2008, and the Ph.D. degree in electrical engineering, in 2018, under the SLAB/SLAI Scholarship. In 2009, she joined UiTM, as a Young Lecturer and promoted as a Senior Lecturer with the School of Electrical Engineering, College of

Engineering, UiTM, Penang Branch, in 2013. Currently, she is with the School of Computer Sciences, USM, as Postdoctoral Fellowship. She is attached to the Department of Control System Engineering at the faculty. She is also a member of the AREDiM Research Group, the Head of the Research Group RIDyLT and actively involved in teaching and learning research. Her research interests include model development using image processing and artificial intelligence.



MUHAMMAD KHUSAIRI OSMAN received the B.Eng. degree in electrical and electronic engineering and the M.Sc. degree in electrical and electronic engineering from the Universiti Sains Malaysia (USM), in 2000 and 2004, respectively, and the Ph.D. degree in medical electronic engineering from the Universiti Malaysia Perlis (UniMAP), Malaysia, in 2014. He is currently a Senior Lecturer with the Faculty of Electrical Engineering, Universiti Teknologi MARA (UiTM), Malaysia. His research interests include image processing, pattern recognition, and artificial intelligence.



MOHD SHAWAL JADIN received the B.Sc. (Hons.), M.Sc., and Ph.D. degrees in electrical and electronic engineering from the Universiti Sains Malaysia (USM), in 2002, 2006, and 2018, respectively. In 2002, he held a position as a Research Officer in electrical power with USM. From 2005 to 2006, he was a Lecturer with UiTM, Malaysia. Since 2006, he has been attached as a Lecturer with the Faculty of Electrical and Electronic Engineering Technology, Universiti Malaysia Pahang Al-Sultan Abdullah, Pahang, Malaysia. His research interests include power electronic and drives, renewable energy, infrared thermography, image processing, bioenergy, hydrogen fuel cell, and condition monitoring.



KAMARULAZHAR DAUD received the bachelor's degree in electrical engineering from the Faculty of Electrical Engineering, Universiti Teknologi MARA (UiTM), Shah Alam, Malaysia, in 2003, the Master of Science degree in electronic system design engineering from the School of Electrical and Electronics Engineering, Universiti Sains Malaysia, in 2006, and the Ph.D. degree in electrical engineering, specializing in power quality from UiTM, in 2019. He is currently a Senior Lecturer with UiTM, Permatang Pauh Campus, Pulau Pinang, Malaysia. His research and teaching interests include theory and application of power quality, high voltage engineering, signal processing, and artificial intelligence-related research.



MOHD ZULHAMDY AB HAMID received the Bachelor of Engineering degree (Hons.) in electrical and electronic engineering from the Universiti Teknologi MARA, Cawangan Pulau Pinang, Malaysia, in 2018, where he is currently pursuing the Master of Science degree in electrical engineering with the Postgraduate Centre of Electrical Engineering Studies. His research is centered on the application of artificial intelligence, with a particular focus on deep learning techniques. He is also exploring advanced methods in digital image processing, including data preprocessing and enhancement, to improve image analysis and interpretation.

...